Rolling Element Bearing Defect Detection and Diagnostics Using REBAM® Probes

Authored by:

Donald E. Bently

Founder, Chairman, and CEO
Bently Nevada Corporation, and
President
Bently Rotor Dynamics Research Corporation
e-mail: don@bently.com

Paul Goldman

Manager
Bently Rotor Dynamics Research Corporation
e-mail: paul.goldman@bently.com

John J. Yu

Research Scientist
Bently Rotor Dynamics Research Corporation
e-mail: john.yu@bently.com

Rolling element bearings are used extensively in many machinery applications. Condition monitoring has the advantages of reducing downtime and improving the maintenance efficiency of such equipment. Thus, it is very important for maintenance engineers to understand the proper techniques and instrumentation used to monitor and diagnose problems associated with rolling element bearing machinery.

Most diagnostic techniques for rolling element bearings entail signature analysis of data from acceleration or velocity transducers mounted on the bearing housing or machine casing [1]. As a result, vibration signals from bearings can be obscured by other components from the associated machinery and foundation. Therefore, Bently [2], Harker and Sandy [3], and Bosmans [4] tested an eddy current transducer known as REBAM® (Rolling Element Bearing Activity Monitor) for this application. Kim [5] also experimented with this type of transducer, but did not discuss how a time-domain representation could show the nature of the outer race deflection associated with bearing frequencies for a bearing with raceway defects. It has often been misconstrued that this type of transducer, measuring outer race displacement only, may not detect an inner race defect. Therefore, Yu et al. [6-8] conducted research that established the relationship of spike signals in outer race deflection to raceway and ball/roller defects.

As shown below, the inner race defect can be readily detected by REBAM® probes. In addition, it is well known that a defect at any element of a rolling element bearing transmits very rapidly to all other elements.

The remainder of this article explains methodologies used to detect inner race, outer race, and rolling element defects using REBAM® probes. Deflection of the outer race in a rolling element bearing is measured directly using this high-gain probe. The relationship of defect influence to the outer race deflection near the probe tip in the time domain is discussed. To better understand the detection techniques, experimental data is presented with simplified equations and explanations. Detection methods for inner race defects are also discussed in depth.

"New detection methodology using the REBAM® probe makes it possible to diagnose inner race defects correctly and the nature and characteristics of the observed signals can be fully understood."

Bearing test rig

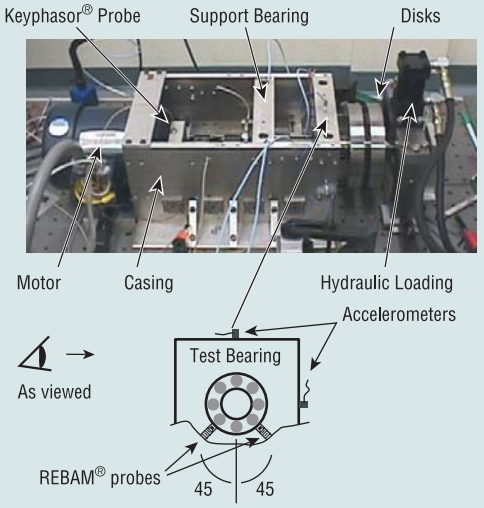

Figure 1.

Approximate ratios of tested bearing frequencies to shaft speed

Approximate ratio of tested bearing frequencies to shaft speed	Ball bearing	Roller bearing
Inner race ball pass: i_{IRBP}	4.9	7.2
Outer race ball pass: i_{ORBP}	3.1	4.8
Rolling element spin: i_R	2.0	2.3
Cage: i_C	0.38	0.39

Table 1.

Outer race deflection at 680 rpm shaft rotative speed measured by REBAM® probe (a) timebase and (b) spectrum

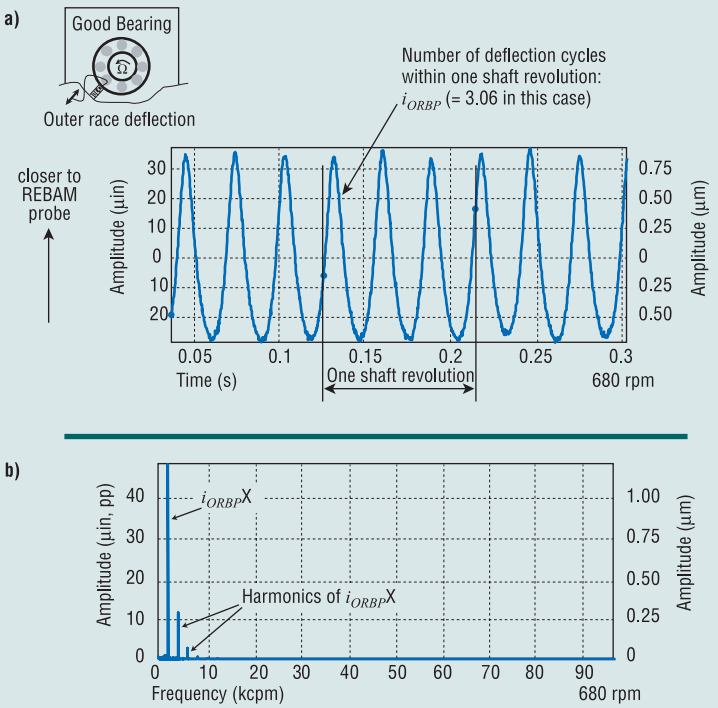

Figure 2.

Test Rig

The test rig used in this study (Figure 1) consists of a rotor with one support bearing and one test bearing and is driven by a 746 W (1 hp) motor.

The shaft is 419 mm (16.5 in) long with diameters varying from 30 mm (1.18 in) to 41 mm (1.6 in). Attached to the shaft are two overhung mass disks, each of 177.8 mm (7 in) diameter and 25.4 mm (1 in) thickness. To compensate for rotor unbalance, a mass is placed in one of several holes located on a disk. A hydraulic pump with a 25.4 mm (1 in) diameter cylinder was used to apply load to the shaft through a roller bearing with a much higher number of elements than the test bearing. This was to ensure that the loading bearing frequencies would not interfere with the test bearing frequencies. Load on the bearing can be varied between –2224 N (–500 lb) and +2224 N (+500 lb), where negative numbers correspond to upward loading and positive numbers correspond to downward loading. Experimental data in this article corresponds to the downward direction. Note that the test bearing is preloaded to some extent, even without hydraulic loading, due to the weight of the mass disks on this overhung rotor. The bearing housings are fixed to the casing, which in turn is fixed to a large concrete foundation.

Casing response at 680 rpm shaft rotative speed in time and frequency domains from accelerometers mounted in (a) vertical and (b) horizontal directions

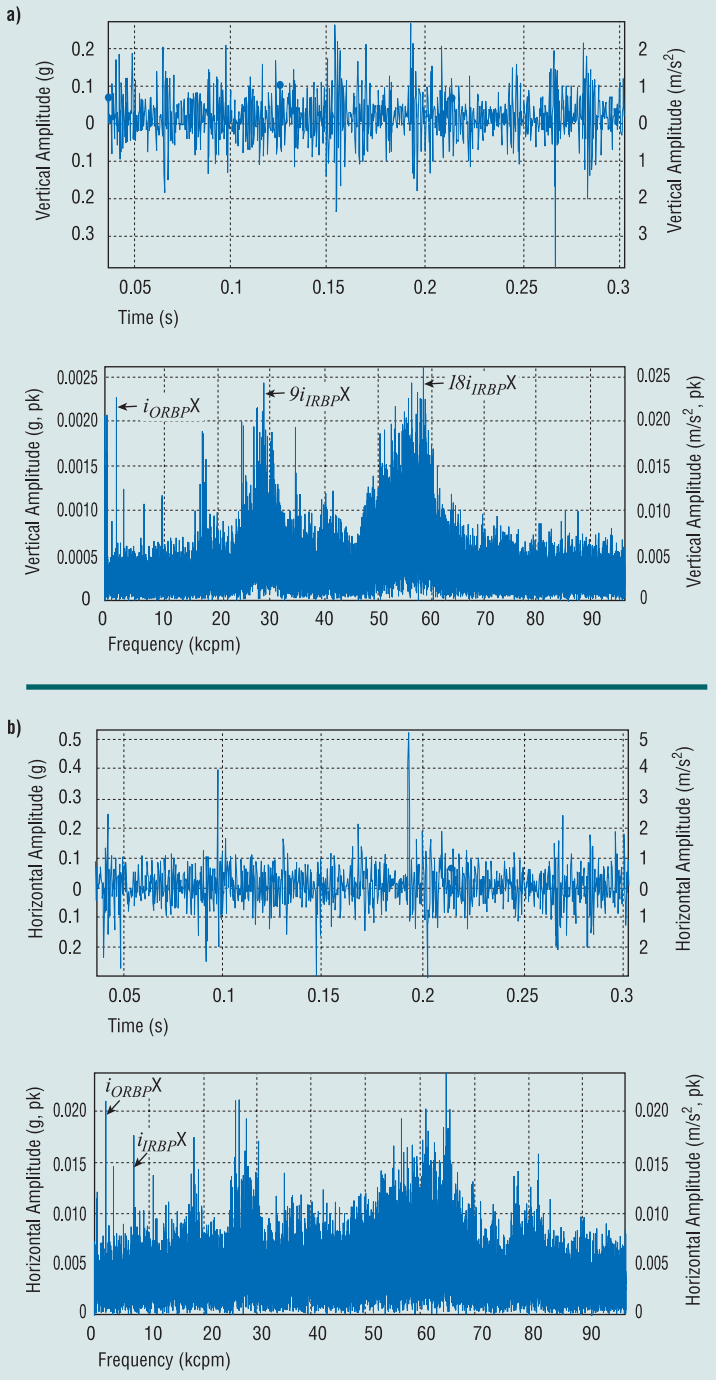

Figure 3.

REBAM® probes, with a gain of 78.7 mV/µm (2 mV/µin) were used to measure the outer race deflection of the bearing. Accelerometers were also mounted on the casing for comparison with the REBAM® probes.

Ball and roller bearings were used for the study of transducer response to raceway and rolling element defects, respectively. Ratios of tested bearing frequencies to shaft speed, based on experimental data from good bearings, are shown in Table 1. Note that these values may change due to defect effects and vary with operating conditions. If a defect occurs on either an inner or outer race, balls/rollers will contact the defect at a frequency of i_{IRBP}X or i_{ORBP}X, where X = shaft rotative speed, IRBP = inner race ball pass, and ORBP = outer race ball pass. The sum of these two ratios is equal to the number of balls/rollers regardless of changes in speed and slip. If there is a defect on a ball/roller, the inner or outer race will contact the defect at a frequency of i_RX. Since a REBAM® probe detects outer race deflection near the probe tip, the frequency ratio (i_C) of the moving cage that holds the balls/rollers is related to the detection of ball/roller defects.

Vibration Signature for Good Bearings

Both high-gain displacement transducers and accelerometers were installed to observe the corresponding vibration signature for a non-defective test bearing. The purpose was to find an effective sensor to accurately monitor the bearing operation and expose bearing defects.

Eddy current REBAM® probes mounted in the holes of the housing can detect very small elastic deflections of the outer race as each rolling element under load passes near the probe tips. This deflection has a cycle of $\frac{360^\circ}{i_{ORBP}}$ shaft rotation. A good bearing exhibits a smooth timebase plot, denoting very little deflection. Figure 2a shows the vibration signature from a REBAM® probe mounted at the location shown. Besides the weight of the entire rotor system, a hydraulic load of 1379

kPa (200 psi) downward is applied at the right end of the shaft as shown in Figure 1. The test bearing has no defects on its inner race, outer race, or balls, and no lubrication is supplied between the balls and raceways.

The localized deflection curve of the outer race, facing the REBAM® probe, is clearly evident in the time domain where the shaft speed is 680 rpm (see Figure 2a). The deflection has peak-to-peak amplitude of about 1.65 µm (65 µin). For each shaft rotation, the number of periodic waveform cycles due to the deflection is equal to i_{ORBP} (= 3.06 in this case). When a ball is located near the point where the REBAM® probe is mounted (left side, 45° from the bottom), the outer race, due to the ball pressing on it, deforms away from the bearing center and toward the probe. This corresponds to all the high peak points in the timebase plot shown in Figure 2a and is the maximum deflection towards the probe. When two adjacent balls are located equidistant from the probe tip, the deflection of the outer race is released and the outer race moves away from the probe. This corresponds to the low peak points in the timebase plot shown in Figure 2a. Due to surface roughness with lack of lubrication, ball tolerances, and ball undulations, there exist slight fluctuations on the deflection curve.

"Compared with REBAM® probes, casing-mounted accelerometers may give misleading indirect data about bearing conditions. Frequency components that correspond to defective bearings exist even for non-defective bearings. Response is largely dependent on the rotor/casing system."

Figure 2b shows the deflection signal in the frequency domain. Outer race ball pass frequency, i.e., the i_{ORBP}X (= 3.06X in this case) component, is dominant, accompanied by its harmonics, 2(i_{ORBP}X), 3(i_{ORBP}X), etc. The synchronous 1X component is almost negligible. Obviously, inner race ball pass frequency, i.e., the i_{IRBP}X (= 4.94X in this case) component, is not apparent in the frequency domain.

Vibration signals from casing-mounted accelerometers include transducer response to rotor unbalance, foundation, and other frequency components in addition to the rolling element bearing operation. Figure 3 shows the signals in both the vertical and horizontal directions for the same operating condition as in Figure 2. Information from the rolling element bearing operation is obscured or masked with the vibration signature from other sources in the rotor/bearing/foundation system. In the timebase plots shown in Figure 3, spikes or impulses occur although no defects exist in the bearing. In the spectrum plots shown in Figure 3, the vibration signals include components of i_{ORBP}X, i_{IRBP}X, and their harmonics for this non-defective bearing. It is known that these components often appear for a defective bearing and for that reason are typically used to identify defects in the bearing. Nevertheless, applying this rule would misdiagnose the bearing. Therefore, it would be difficult to distinguish between defective and non-defective bearings by simply observing these fault frequency components with accelerometers, especially as the response is greatly dependent on the casing. The harmonics of these bearing frequencies may or may not generate detectable casing vibrations. Although the number and magnitude of these components may be higher, as observed during experiments, it would be hard to establish a quantitative criterion for determining whether a bearing is damaged or not.

These tests clearly indicate that the REBAM® probe detects only the deflection of the outer race of the rolling element bearing. If a deflection in the rolling element bearing is related to a defect, a detection technique using the REBAM® probe will be successful. Note that even for a good bearing without outer race defects, the spectral data of the deflection detected by the probe still gives the i_{ORBP}X component and its harmonics. No i_{IRBP}X component is present in the spectrum. However, as will be discussed, defects occurring in the inner race, the outer race, or a rolling element can be successfully detected by the REBAM® probe.

Detection of Bearing Defects

As discussed previously, the outer race is deflected towards the REBAM® probe each time an element under load passes by the probe location. This produces a positive change in the displacement, relative to the low peak of the deflection curve where the least loading acts on the outer ring facing the probe. For spalling defects,

material is actually removed from the raceway or ball/roller surface. This defect produces a location of increased clearance, and ball/race contact at the defect is actually unloaded temporarily over a very short time period. This unloading makes the outer race spring back away from the REBAM® probe, resulting in a short duration spike in the timebase waveform.

Inner Race Defect

Detection of an inner race defect is often considered a difficult task when monitoring rolling element bearings. It is sometimes incorrectly assumed that displacement transducers such as REBAM® probes cannot detect inner race defects. Although some spikes may have been observed, the nature of these signals had not been fully examined when applying high-gain displacement transducers. Thus, it was difficult to diagnose the occurrence of inner race defects and distinguish them from other defects.

New detection methodology using the REBAM® probe makes it possible to diagnose inner race defects correctly, and the nature and characteristics of the observed signals can be fully understood. The accompanying real data validates this detection methodology.

Detection Methodology

If a defect occurs in the inner race, it will contact the rolling elements i_{IRBP} times on average during each shaft rotation. The REBAM® probe detects negative spikes when the moving defect is located within an

Diagram of inner race defect detection methodology using REBAM® probe

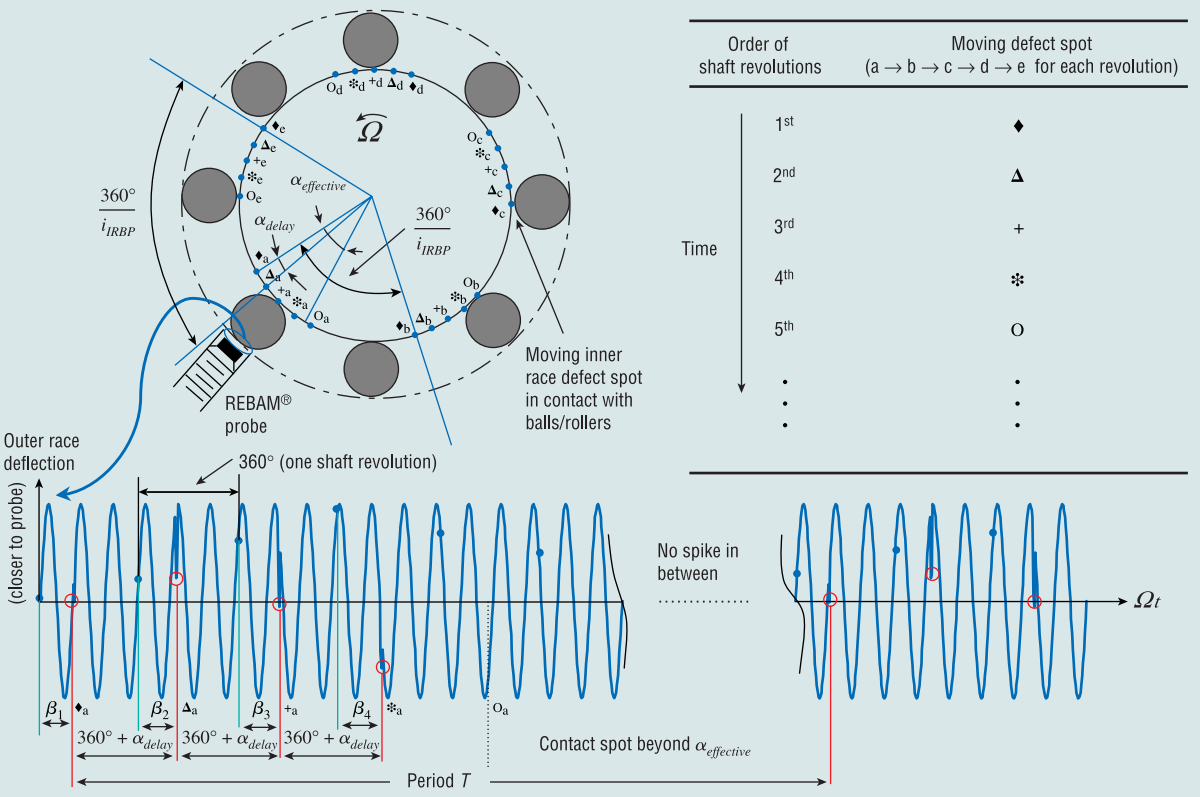

Figure 4.

effective zone near the probe. Figure 4 shows a diagram of the defect detection methodology and assumes that one defect occurs on the inner raceway.

Suppose that at one time (in the first shaft revolution), the defect in contact with a ball is entering the effective zone $\alpha_{effective}$ in which the probe can detect the negative spikes. A negative spike will occur in the effective zone, marked with "$\blacklozenge_a$". This is also denoted in the timebase plot with the same symbol. After $\frac{360^\circ}{i_{IRBP}}$ degrees of shaft revolution from "$\blacklozenge_a$", where the defect contacts the next ball at "$\blacklozenge_b$", the probe cannot detect a negative spike because the contact occurs beyond its effective zone. For the following contact at "$\blacklozenge_c$", the same situation occurs where the event is again outside the REBAM® effective zone. This situation exists until the defect contacts the j^{th} (j is a round number for i_{IRBP}) ball within the effective zone again, as is indicated by "Δ_a." Note that two conditions must be met for the probe to detect these negative spikes. One is that the inner race defect must contact the balls and the other is that the defect contact must be within the effective zone.

In the timebase plot, the two adjacent negative spikes between "$\blacklozenge_a$" and "Δ_a" have, in terms of shaft rotations (degrees), an interval of

$$\alpha_{IR} = Round\left(i_{IRBP}\right)\frac{360^\circ}{i_{IRBP}} \qquad (1)$$

A delay angle between the two contact areas within the effective zone "$\blacklozenge_a$" and "Δ_a" is

Relation between i_{IRBP} and detected spike group period T

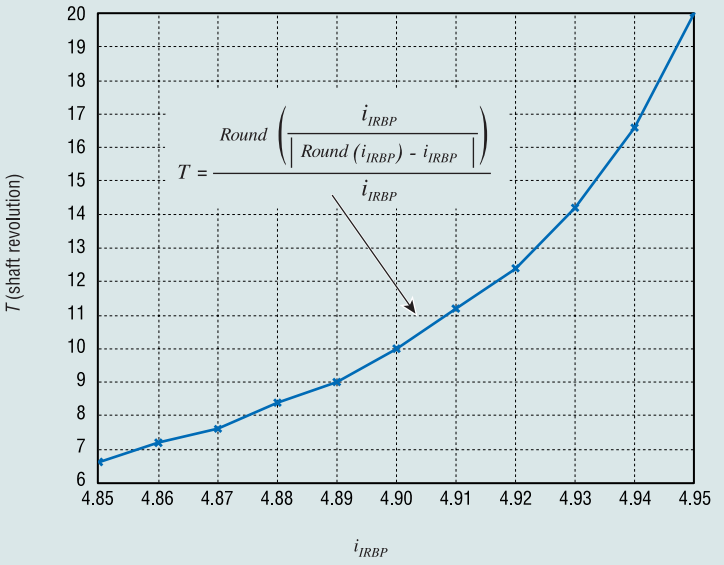

Figure 5.

$$\alpha_{delay} = \alpha_{IR} - 360^\circ = \left[Round\left(i_{IRBP}\right) - i_{IRBP}\right] \times \frac{360^\circ}{i_{IRBP}} \qquad (2)$$

where *Round* (i_{IRBP}) represents a round number for i_{IRBP} (for example, *Round* (4.9) = 5, *Round* (4.1) = 4). In Figure 4, the defect contact area moves "forward" (from "$\blacklozenge_a$" to "Δ_a", the same direction as Ω) within the effective zone as α_{delay} is assumed to be greater than zero in this case. It would move "backward" in the case of $\alpha_{delay} < 0$.

The interval α_{IR} will be longer than 360° shaft rotations for $\alpha_{delay} > 0$ and shorter for $\alpha_{delay} < 0$.

For the 3rd and 4th shaft revolutions, the scenario will be similar to that for the 1st and 2nd revolutions, as marked with "+" and "∗" symbols. For the 5th shaft rotation, since the defect contact, (marked with "O_a"), is beyond the effective zone, no spikes will be shown in the timebase plot.

This no-spike situation in the timebase plot will remain until the defect contact area on the left side (marked with subscript "e" in Figure 4) moves into the

"It is sometimes incorrectly assumed that displacement transducers such as REBAM® probes cannot detect inner race defects."

effective zone, thus making another similar cycle as discussed above. From Figure 4, such a spike group cycle T can be expressed in terms of shaft revolutions as $T \approx \frac{360^\circ}{i_{IRBP}} \Big/ |\alpha_{delay}| = \frac{1}{Round(i_{IRBP}) - i_{IRBP}}$. Since the defect spot contacts a ball with a cycle of $\frac{360^\circ}{i_{IRBP}}$ shaft rotation, the expression $360^\circ\ T = n\frac{360^\circ}{i_{IRBP}}$ holds where n is an integer. It follows that $n = Round\frac{i_{IRBP}}{Round(i_{IRBP}) - i_{IRBP}}$. Thus the cycle T is

$$T = \frac{n}{i_{IRBP}} \frac{Round\left(\frac{i_{IRBP}}{|Round(i_{IRBP}) - i_{IRBP}|}\right)}{i_{IRBP}} \quad (3)$$

shaft revolutions.

Note that a slight change in i_{IRBP} causes a much bigger change in detected spike group cycle T, as shown in Figure 5. Therefore, a change in i_{IRBP}, which is related to slip, can be more accurately estimated from T.

During the cycle T in the time domain, the number of consecutive spikes n_{spike} is approximately equal to $n_{spike} \approx \frac{\alpha_{effective}}{\alpha_{delay}}$. Assume that the effective zone is symmetric about the probe location and the Keyphasor® mark is aligned with the probe. Thus, from Figure 5, the location of the inner race defect (in terms of shaft orientation) can be estimated by

$$\beta_{defect} \approx \frac{1}{n_{spike}} \sum_{i=1}^{n_{spike}} \beta_i \quad (4)$$

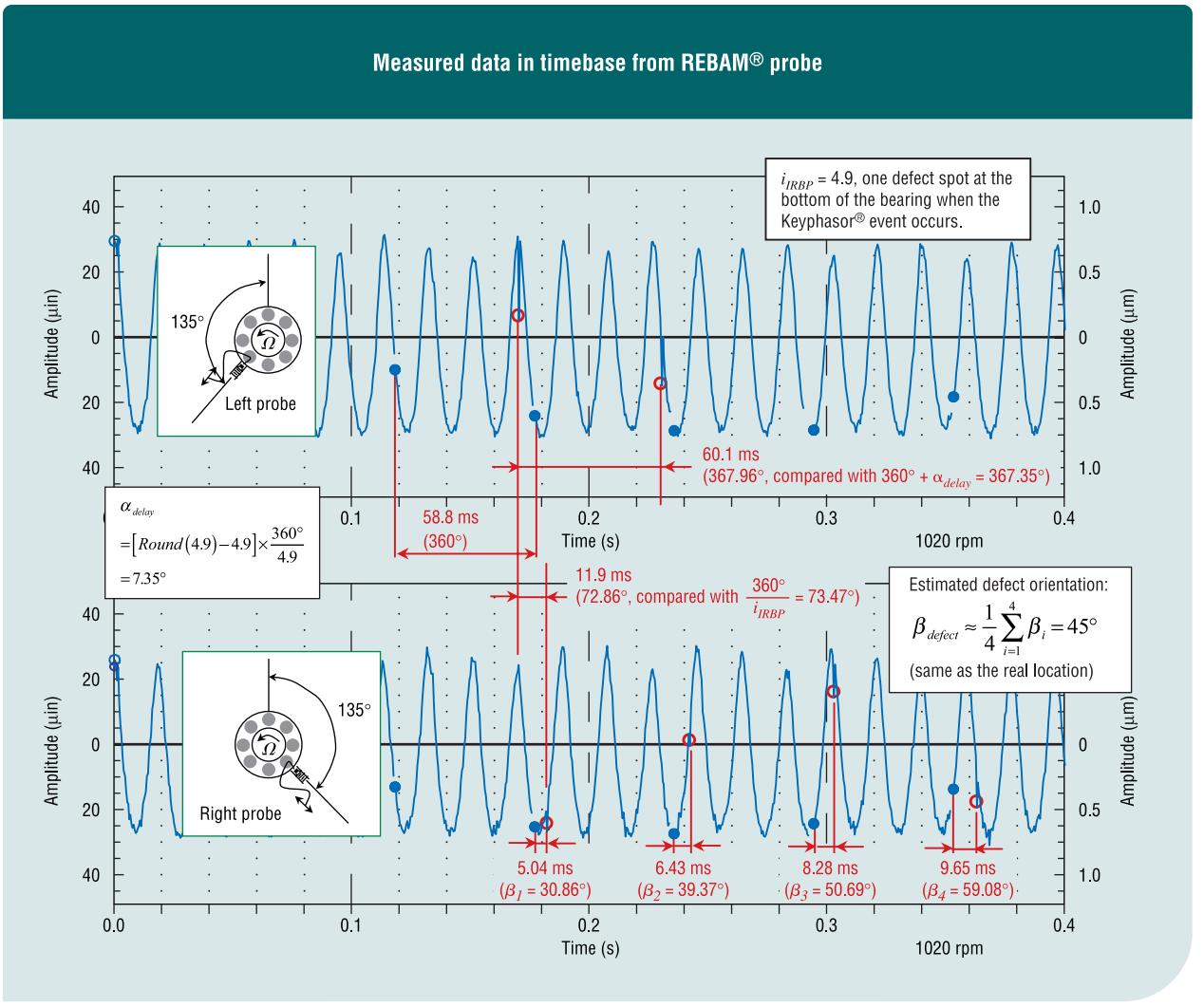

Figure 6.

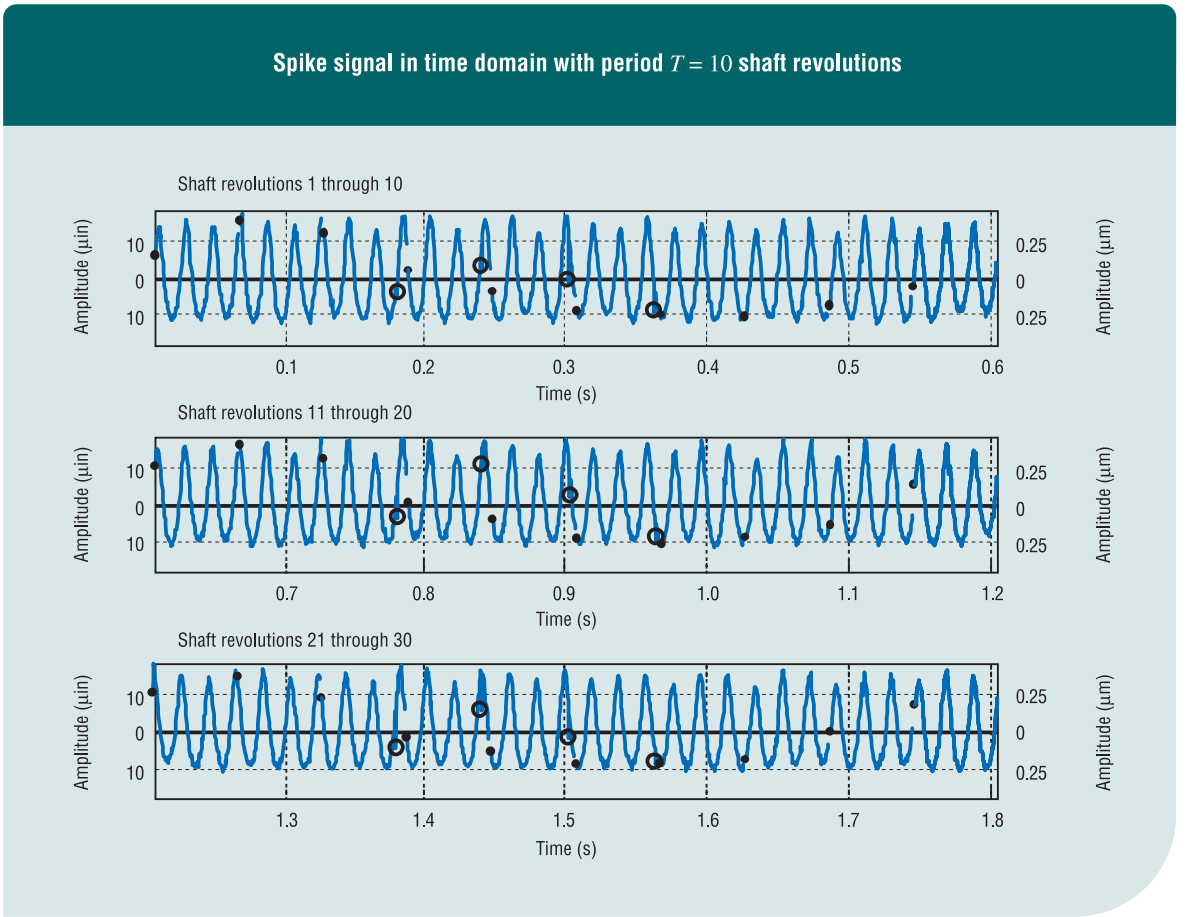

Figure 7.

where β_{defect} is a shaft rotational angle delayed relative to the probe aligned with the Keyphasor® mark.

If two probes are configured at an angle which allows two defect contact events to occur within their effective zones, spikes will appear in their corresponding timebase responses, with an interval of $\frac{360^\circ}{i_{IRBP}}$ rotation within a single shaft revolution. The additional probe was used to confirm an inner race defect in the study. In the field, however, having one probe is sufficient to identify the defect.

Real Data Analysis

For the test ball bearing, an artificial spall was made on the inner race and oriented on the shaft so that the defect would be at the bottom of the bearing (180° from top) when the Keyphasor® pulse was triggered. The ratio of inner race ball pass frequency to shaft speed (i_{IRBP}) was found to be 4.9 (which could be determined from i_{ORBP} in the frequency domain, or more accurately from T). Therefore, according to Equations (1) and (2), the two adjacent negative spikes should have an interval of

$$\alpha_{IR} = Round\left(i_{IRBP}\right)\frac{360^\circ}{i_{IRBP}} = 367.35^\circ > 360^\circ$$

in terms of shaft rotation Ωt, and the delay angle within the detectable zone should be

$$\alpha_{delay} = \left[Round\ (4.9) - 4.9\right] \times \frac{360^\circ}{4.9} = +7.35^\circ \text{ (moving forward).}$$

Such a phenomenon should repeat, according to Equation (3), with a cycle of

$$T = \frac{Round\left(\dfrac{4.9}{Round\,(4.9) - 4.9}\right)}{4.9} = 10 \text{ shaft revolutions.}$$

Figure 6 shows experimental data from the REBAM® probes for this case. A hydraulic force of 943 N (212 1b) was applied to the non-drive end of the shaft; rotor speed was about 1020 rpm. In the time domain, a

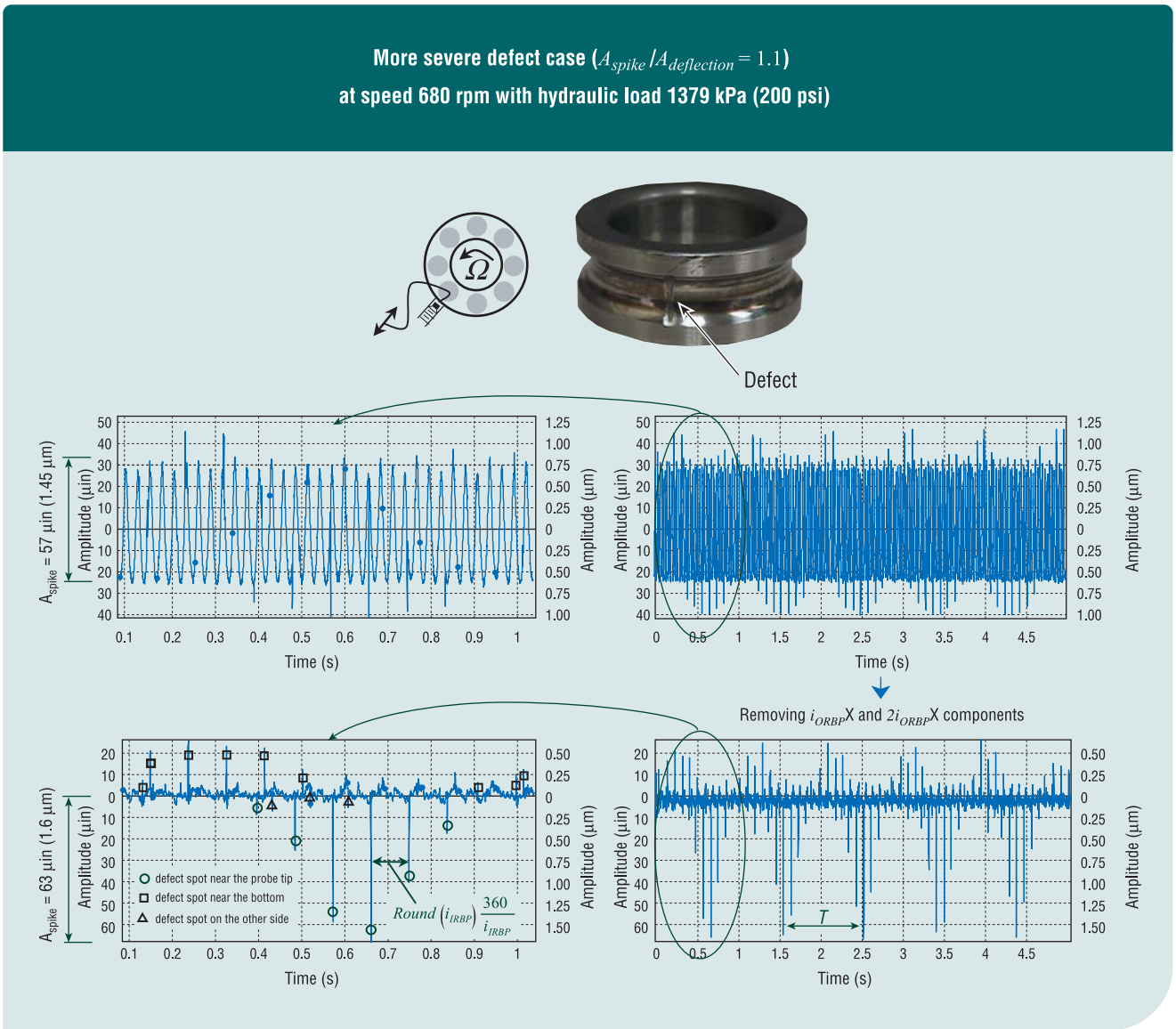

Figure 8.

time period of 58.8 ms within the two adjacent Keyphasor® dots corresponds to one complete shaft revolution (rotation of 360°). Based on this ratio, two negative spikes separated by 60.1 ms have an interval of 367.96°. This is very close to the expected value of α_{IR} = 367.35°. The right probe first detects a spike 72.86° (11.9 ms) later than the left probe, which is also in agreement with the expected value of $\frac{360^{\circ}}{i_{IRBP}}$ = 73.47°.

Note that only 128 data samples were taken for 360° shaft rotation in this case.

Using Equation (4) along with the given β_i values in the timebase for the right probe (Figure 6), the location of the defect can be estimated using the following:

$$\beta_{defect} \approx \frac{1}{4}\sum_{i=1}^{4}\beta_i = \frac{1}{4}\left(30.86^{\circ} + 39.37^{\circ} + 50.69^{\circ} + 59.08^{\circ}\right) = 45^{\circ}$$

This indicates that the defect had a phase delay relative to the right probe, which was precisely the real defect location.

Figure 9.

For the same defective bearing, probe data in the time domain was recorded over a longer time span to observe the cycle of spike occurrence. Figure 7 shows the left REBAM® probe data for 30 shaft revolutions. As expected, the timebase deflection curve shows a negative spike in each of four consecutive shaft revolutions. In the time intervals before and after the rotations with the spikes, the deflection curve looks normal without obvious defect spikes. This is due to the defect spike event moving in and out of the effective zone in subsequent rotation sequences. This phenomenon repeats itself every 10 shaft revolutions.

Severity Analysis

Given that a bearing may run at various speed and load conditions, spike signals as well as the deflection response can vary. As speed increases, the enhanced centrifugal forces on the balls along with the expansion of the inner race results in tight contact between the balls and raceways. While loading increases, high pressure is maintained between the raceway and the balls. As a result, the outer race deflection and spike amplitude are increased, and smoothness of the deflection curve is greatly increased. Therefore, higher speed and load conditions make spike signals more noticeable. Spike signals, reflecting the occurrence of a defect, are still present in the timebase plot at low speed and under light load, although they are not as pronounced. Removing the i_{ORBP}X and $2i_{ORBP}$X components related to normal loading deflection makes the spikes more pronounced without influencing their magnitude. For a given defect, the ratio of spike-to-deflection amplitude seems to have little change.

Figure 8 shows a more severe inner race defect case. The defect is located at the horizontal position (90° from 0°) when the Keyphasor® signal is triggered. The left REBAM® probe detects the corresponding response in the time domain. Spikes due to the defect become much more pronounced after removing the i_{ORBP}X and $2i_{ORBP}$X components related to normal loading deflection. For this severe case, more negative spikes are present as the defect contact area passes near the probe tip. The spike-to-deflection amplitude ratio is

$$A_{spike} / A_{deflection} = 63/57 = 1.1$$

In this instance, positive spikes also appear. This is because the severe defect contacts a ball near the bottom, where the maximum loading is located. Thus, balls at other contact locations, including the one near the probe tip, are impacted. Notice that small negative spikes occur due to a sudden loose contact when the defect is on the right side.

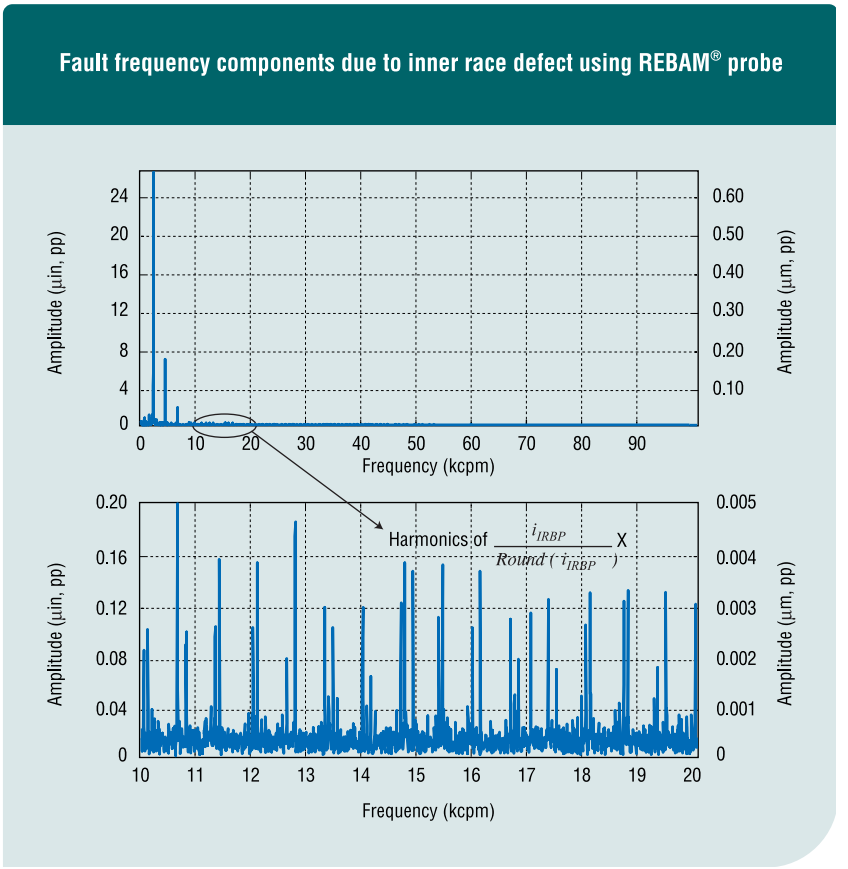

Figure 10.

For the same defect as in Figure 8, increases in speed yield slight increases in deflection amplitude $A_{deflection}$ and spike amplitude A_{spike}. As is expected, hydraulic loading is linearly proportional to the deflection amplitude $A_{deflection}$. It was found that the spike group period T varied from 10 to 13 shaft revolutions (corresponding to approximately i_{IRBP} = 4.90 to 4.92) with changes in speed from 680 to 2040 rpm and hydraulic load from 0 to 2068 kPa (300 psi). These variations are due to slippage between the raceway and balls, which could be estimated. Regardless of changes in speed and load, the ratio $A_{spike}/A_{deflection}$ remains almost the same (≈1.1).

For a less severe defect, as in Figure 9, the ratio $A_{spike}/A_{deflection}$ is decreased to around 0.4. Therefore, this ratio can be used to measure defect severity.

Fault Frequency Components

For spikes with an interval of $Round\left(i_{IRBP}\right)\dfrac{360°}{i_{IRBP}}$ shaft rotation in the time domain, the corresponding multiple harmonic components of $\dfrac{i_{IRBP}}{Round\left(i_{IRBP}\right)}$X can be seen in the spectrum. Figure 10 shows these harmonics associated with the spike signals due to the inner race defect in Figure 9. At 680 rpm, a frequency range of 10~20 kcpm is divided by about 15 intervals with harmonics of $\dfrac{i_{IRBP}}{Round\left(i_{IRBP}\right)}$X $\left(= 0.98\ \text{X}\right)$ for i_{IRBP} = 4.9 · Observing whether these fault frequency components occur is an additional tool to diagnose inner race defects.

Outer Race Defect

An outer race defect in contact with balls/rollers does not move against the probes for a rolling element bearing with its outer ring fixed to the casing. Figure 11

Outer race defect signal measured with REBAM® probe at speed 680 rpm without hydraulic loading: a) timebase and b) spectrum

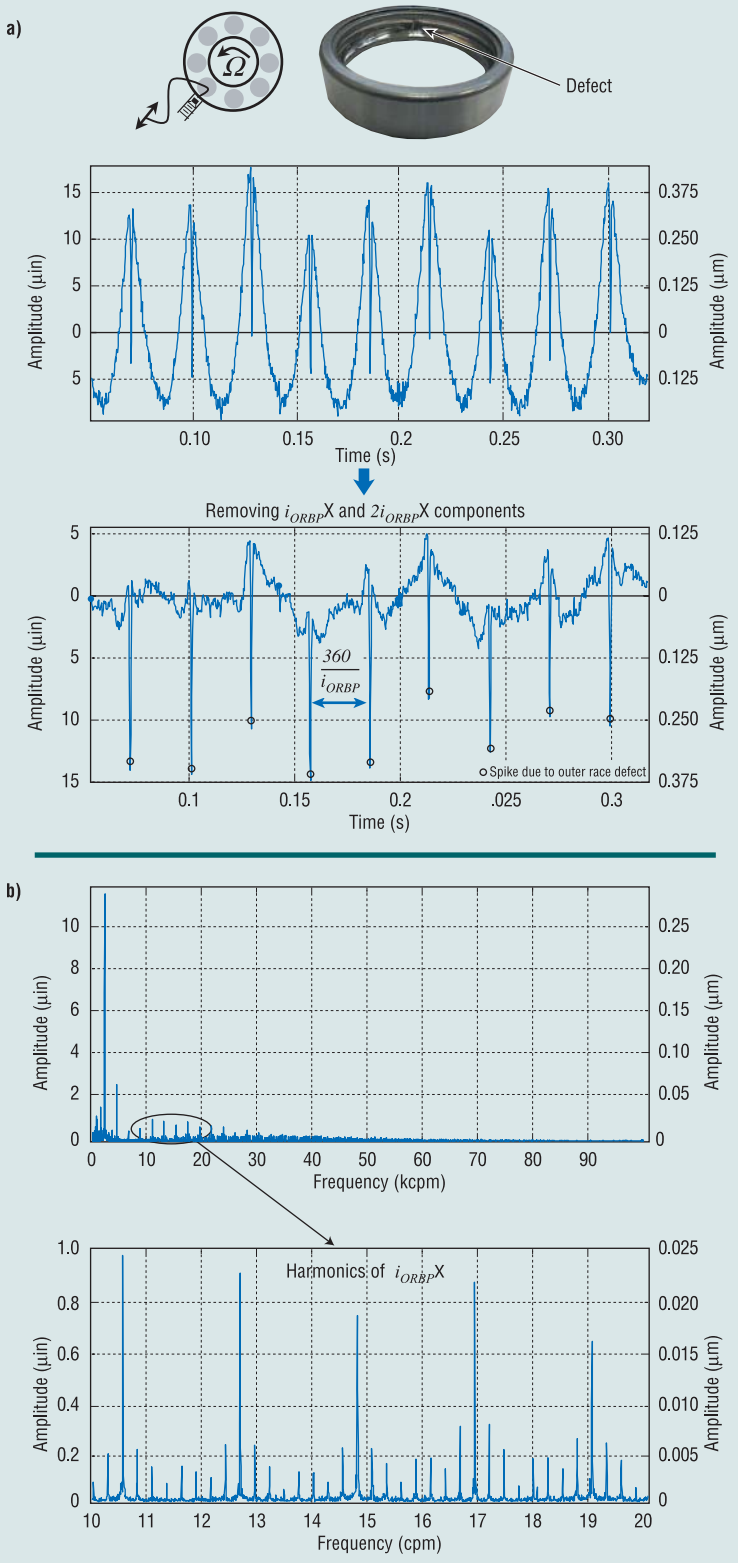

Figure 11.

shows an outer race defect at 680 rpm with 1379 kPa (200 psi) hydraulic loading. Since the defect faces the left probe, a sudden release in pressure between the races and the passing ball leads to a negative spike on the outer race deflection curve. The number of spikes is the same as that of the deflection cycles in time base and the spike interval due to an outer race defect is

$$\alpha_{OR} = \frac{360^\circ}{i_{ORBP}} \tag{5}$$

Therefore, the fundamental frequency of spikes due to an outer race defect is equal to that of the outer race deflection; i.e., i_{ORBP}X. Due to the defect, many of its harmonics are seen in a frequency range higher than $3i_{ORBP}$X. Since ball sizes vary, harmonics of the cage (holding all the balls) frequency $i_C\text{X}\left(=\frac{1}{8}i_{ORBP}\text{X}\right)$ are also present as side bands.

It is found that spike magnitude and direction (positive or negative) due to an outer race defect varies with the defect orientation, as shown in Figure 12. Numbers on the bearing indicate outer race defect orientations and correspond to the numbered spikes on the deflection curves. Spike magnitudes and directions are also marked. The response for defects on the right side can be figured out, based on Figure 12. These areas cover most of the loading zone where outer race defects usually occur. For a severe defect facing the probe, the fundamental frequency component i_{ORBP}X can decrease if the defect faces the probe, as in position "1," and can increase if the defect is at the bottom where maximum load is located, as in position "5." However, many of its harmonics in the order higher than $3i_{ORBP}$ will become more pronounced than those without the defect. Having two probes is helpful to determine the defect orientation and severity.

Rolling Element Defect

If a rolling element (ball/roller) defect occurs, it will contact both the inner race and the outer race at its spin frequency $2i_R$X. A negative spike will be detected when the defect on the damaged ball/roller, which is held by the cage rotating at frequency i_CX, contacts either the inner race or the outer race within the effective zone near the probe. Assume the probe detects spikes after k events of defect/raceway contacts. Thus, the

Spike signal varying with defect orientation

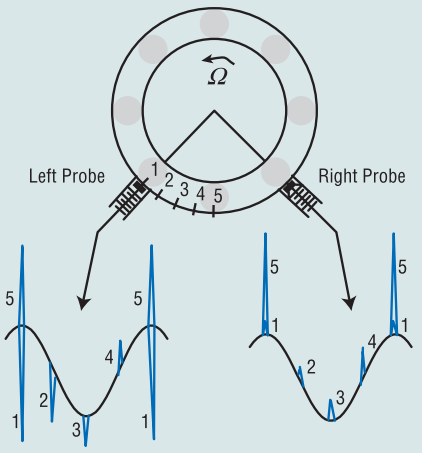

Figure 12.

expression $\frac{360^\circ}{i_C} \approx k\,\frac{360^\circ}{2i_R}$ holds where k is an integer. It follows that $k = Round\left(\frac{2i_R}{i_C} \pm 0.5\right)$. Spike intervals due to a rolling element defect, detected by the probe in timebase, are

$$\alpha_{RE} = k\,\frac{360^\circ}{2i_R}\,Round\left(\frac{2i_R}{i_C} \pm 0.5\right)\frac{360^\circ}{2i_R} \text{ shaft rotations.} \tag{6}$$

Within the effective zone, real locations of defect contacts detected by the probe have intervals of

$$\begin{aligned}\alpha_{FB} &= \alpha_{RE}i_C - 360^\circ \\ &= Round\left(\frac{2i_R}{i_C} \pm 0.5\right)\frac{360^\circ}{2i_R}i_C - 360^\circ\end{aligned} \tag{7}$$

"Most diagnostic techniques for rolling element bearings entail signature analysis of data from acceleration or velocity transducers mounted on the bearing housing or machine casing [1]. As a result, vibration signals from bearings can be obscured by other components from the associated machinery and foundation."

Rolling element defect signal detected by REBAM® probe at 700 rpm with 1379 kPa (200 psi). a) timebase after removing i_{ORBP}X and $2i_{ORBP}$X components along with corresponding defect contact locations near the probe, and b) spectrum.

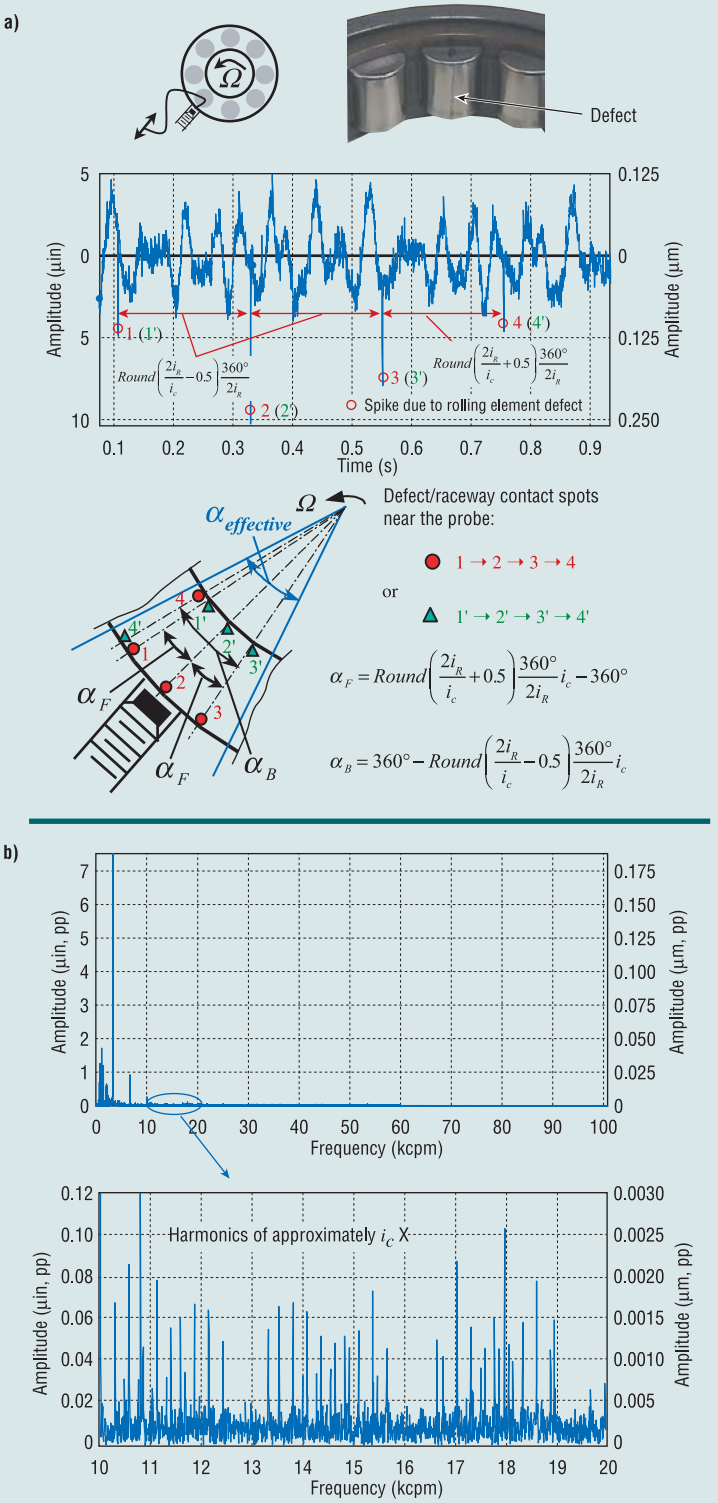

Figure 13.

The locations will move "forward" in the case of $\alpha_{FB} > 0$, and "backward" in the case of $\alpha_{FB} < 0$. An even number of k indicates that two contacts are on the same race, while an odd number means two contacts are on the different races. For spikes with intervals given by Equation (6), many of the harmonics of approximately i_CX are present in its corresponding frequency domain. Figure 13 shows a roller defect that is successfully detected in the time domain as well as in the frequency domain.

Conclusions

Inner race, outer race, and rolling element (ball/roller) defects, which often occur sequentially, can be successfully detected by directly measuring outer race deflection with REBAM® probes. The defect signal is clearly present with spikes in the timebase deflection near the probe tip, but without casing influence, which would be inevitable with case mounted accelerometers. Deflection amplitude is linearly proportional to radial load; an increase in speed results in a slight increase in deflection amplitude. Spike amplitude due to defects usually varies with load and speed in the same way as deflection amplitude. Removing the i_{ORBP}X and $2i_{ORBP}$X components due to outer race deflection makes the spikes more evident. From the experimental data collected in this study, the following conclusions can be drawn:

1. For an inner race defect, negative spikes are seen in several consecutive shaft revolutions with an interval, and then disappear intermittently or become positive, with a spike group cycle T. These parameters are uniquely determined by the inner race ball pass frequency ratio i_{IRBP}. A slight change in i_{IRBP}, which is related to slip, can be more accurately estimated from the corresponding big change in T. For a severe inner race defect, positive spikes appear along with more negative ones.

2. For an outer race defect, a spike occurs in each deflection cycle at a rate of outer race ball pass frequency i_{ORBP}X. The spike amplitude and direction (positive or negative) vary with the defect location relative to the probe. Having two probes is helpful to determine the defect location and severity.
3. For a rolling element (ball/roller) defect, spike intervals are related to not only rolling element spin frequency ratio i_R but also cage frequency ratio i_C. Spikes occur at an average rate of cage frequency i_CX in the time domain.
4. Defect severity can be determined by spike-to-deflection amplitude ratio, which remains almost the same regardless of load and speed changes.
5. Defect locations in the raceway can be determined from spike locations in the time domain, along with the known probe orientation.
6. Defect signals detected from REBAM® probes can also be seen in the frequency domain. Inner race, outer race, and rolling element defects are characterized with harmonics of

$$\left[\frac{i_{IRBP}}{Round\left(i_{IRBP}\right)}\right]$$ X, i_{ORBP}X, and i_CX, respectively.

7. For a defect that happens when metal adheres to the races or rolling elements, i.e., a "bump" instead of a "valley", spike directions would be opposite to those discussed above.

Installed probes measuring the outer race deflection can be used to monitor the load conditions, such as changes in load zones and magnitudes.

Compared with REBAM® probes, casing-mounted accelerometers may give misleading indirect data about bearing conditions. Frequency components that correspond to defective bearings exist even for non-defective bearings. Response is largely dependent on the rotor/casing system.

References:

1. Mathew, J. and Alfredson, R.J., "The Condition Monitoring of Rolling Element Bearings using Vibration Analysis," Transactions of the ASME, *Journal of Vibration, Acoustics, Stress and Reliability in Design,* Vol. 106, 1984, pp. 447-453.
2. Bently, D.E., "Monitoring Rolling Element Bearings," *ORBIT,* Vol. 3 No. 3, November 1982, Bently Nevada Corporation.
3. Harker, R.G., and Sandy, J.L., "Rolling Element Bearing Monitoring and Diagnostics Techniques," Transactions of the ASME, *Journal of Engineering for Gas Turbines and Power,* Vol.111, 1989, pp. 251- 256.
4. Bosmans, R., "REBAM® – Getting Past the Limitations of Seismic Transducers to a More Thorough Root Cause Analysis of a Rolling Element Bearing Failure," *ORBIT,* Vol. 20 No. 1, 1999, Bently Nevada Corporation.
5. Kim, P.Y., "A Review of Rolling Element Bearing Monitoring (III): Preliminary Test Results on Eddy Current Transducer Technique," *Proceedings of Third International Conference on Vibrations in Rotating Machinery*, The Institution of Mechanical Engineers, York, England, 1984, pp. 119-125.
6. Yu, J.J., Bently, D.E., Goldman, P., and Dayton, K.P., "Detection of Rolling Element Bearing Defects in Time Base," Bently Rotor Dynamics Research Corporation, *BRDRC Report 1*, 2000.
7. Yu, J.J., Bently, D.E., Goldman, P., Dayton, K.P., and Van Slyke, B.G., "Rolling Element Bearing Defect Detection and Diagnostics Using Displacement Transducers," *ASME Paper 2001-GT-28*.
8. Yu, J.J., Bently, D.E., Goldman, P., and Dayton, K.P., "Detection of Rolling Element Bearing Defects," *ASME Paper FEDSM 2001-18089*.